



Thermodynamic quantities of magnetised PNJL model in non-zero chemical potential

ANJU DAHIYA¹, K K GUPTA² and S SOMORENDRO SINGH^{1,*}

¹Department of Physics and Astrophysics, University of Delhi, Delhi 110007, India

²Department of Physics, Ramjas College, University of Delhi, Delhi 110007, India

*Corresponding author. E-mail: sssingh@physics.du.ac.in

MS received 28 August 2021; revised 9 June 2022; accepted 8 July 2022

Abstract. The recent research work of two-flavor quarks with magnetised Polyakov–Nambu–Jona–Lasinio (mPNJL) model has been upgraded with the inclusion of a finite chemical potential in the temperature-dependent quark mass and the chemical potential in the interaction potential of Lagrangian density in continuation of the work of Dahiya and Singh (*Pramana – J. Phys.* **94**:120 (2020)). The thermodynamic quantity like equation of state (EOS) and its relevant thermodynamic properties after the inclusion of the finite chemical potential in the temperature-dependent quark mass and potential are represented in the results. The outputs from the calculations show that all the thermodynamic quantities are obtained in such a way that it is enhanced and improved from the earlier result of thermodynamic properties of zero chemical potential. It means that the chemical potential really plays the role of upgradation in the outputs of thermodynamic parameters in comparison to the output produced by the absence of chemical potential in the thermal mass and potential of the Lagrangian density.

Keywords. Quantum chromodynamics; quark-gluon plasma.

PACS Nos 25.75.Ld; 12.35.Mh

1. Introduction

In high-energy heavy-ion collisions, it has been found that it is an interesting research area since last two decades for the high temperature scale. The study in this area has given a very important and significant understanding to the families of theoretical and experimental groups of particle, nuclear and astrophysics. As it is the theory of strong interactions called quantum chromodynamics (QCD), the interaction is of short range and studying it deals with perturbative and non-perturbative features of QCD. Studying the perturbative part is not difficult whereas non-perturbative part is highly complicated. So the effect produced by non-perturbative features can be studied through the thermal excitation at high temperature and baryon chemical potential. At high temperature and nuclear density, QCD is of asymptotic nature in which the component parts of the matter are free quarks and gluon as the bound hadrons melts into a deconfined phase. In this QCD phenomena, there is a separation between these two matters, where one phase is obtained at a much lower temperature called hadronic matter of bound quarks and the other at very

high temperature called deconfined matter of free quarks and gluons called quark gluon plasma (QGP). However, it is believed that the matter is found to coexist with a short span of life of a mixed phase in which the temperature is found to be around (150–250) MeV and then subsequently cooled down the system, and it becomes completely a hadronic phase. In addition, recently a particularly interesting phenomenon of rich baryonic matter has been discussed in some laboratories [1] and that laboratories also focus on finding the structure of the QCD phase. From this information, we get the motivation to study the QCD phase structure at finite temperature T and chemical potential μ . However, the possible critical temperature about the phase transition can be determined from the QCD phase diagram. The structure determines the possible order of phase transition depending on the temperature. In support of these studies, groups at Large Hadron Colliders (LHC) at CERN try to find out the QGP signature after doing a number of experiments with collisions of heavy ions. However, these experiments explain the involvement of huge magnetic field as the accelerated charged particles carry the magnetic field. So the QCD phase

structure is modified with the involvement of magnetic field, in drawing the QCD phase boundary between the bound hadronic phase and unbound matter of hot soup of free quarks and gluons. In addition to it, it will theoretically support the signal of QGP formation [2]. It is also believed that the transition takes place during the early phase of Universe evolution, and the evolution of Universe can also be reproduced in contemporary heavy-ion collision experiments as colliding heavy-ions of Pb-Pb/Au-Au nuclei producing a state of matter as mini-Universe called quark gluon plasma (QGP). So there are many experiments around the globe that try to prove the existence of QGP. It also claimed that the study had proved the existence of QGP at RHIC at BNL and SPS at CERN. From these experimental proofs, the curiosity on the study of QGP formation has expanded thoroughly for the last two decades and it can be signified from different angles of signatures, viz., photon/dilepton production, strange enhancement, hydrodynamical studies and QCD phase structure like equation of state (EOS) [3]. However, it indicates that the interacting matter of hot plasma behaves like an ideal relativistic fluid and hence the matter can be described by relativistic hydrodynamics [4]. This information implies that QGP fluid is highly complicated. To describe such a complicated and crucial aspect, we need the relationship between local thermodynamic quantities and the EOS. The evaluation of EOS is mainly focussed on two important parameters, temperature T and chemical potential μ , of the phenomenologically created free quarks and gluons [5]. Therefore, a sharp transition is expected to occur from a bound hadronic matter to an unbound state of QGP called a deconfined state of non-interacting free particles of quarks and gluons. So, the centre symmetry in QCD is broken due to the availability of these free quarks as they move around. Moreover, many models exist to study these phase transitions. Two of them are the Polyakov–Nambu–Jona–Lasinio (PNJL) model and a combination of the chiral linear-sigma model and the Polyakov loops (PLSM) [6,7]. These models offer theoretical framework to study some properties of QGP. However, these works tackle the possible change in properties of QGP when the strongly interacting system goes through a phase transition between hadronic and partonic phases and it also reported about the effects of transition temperature by the magnetic field [8]. So, in this case, the colour interactions will be the dominant components which can be achieved by increasing the Polyakov loop fields. Obviously, each of them equips us with a different understanding about the critical temperature under the effect of an external magnetic field [9]. Nevertheless, the Polyakov loop remains small up to a particular temperature and then it increases very fast during a small

interval of temperature difference. Due to these effects, there is an overlap in the calculation of energy density denoting abrupt change in the degree of freedom of the system. So, there is an imbalance in the degree of freedom between these two phases. Besides these ideas, if a Polyakov loop parameter of the magnetic field is considered, then there is entanglement in the PNJL model and due to this, there is a probable rise in magnitude of the magnetic field and enhancement of the Polyakov loop leads to the entangled behaviour. This entanglement leads to the creation of inverse magnetic field catalysis/effect (IMC) in the lattice QCD calculations. However, the effects of magnetic field lead to the condensation of quarks which in turn lead to the rise in the transition temperature for chiral symmetry restoration [10]. So, the determination of the QCD EOS and other thermodynamical quantities are extremely important to the phenomenology of hot and dense nuclear matter in the presence of these magnetic fields. To get all these information, the lattice gauge theory is used as the most competent and reliable method at very high temperature [11]. Therefore, the characteristic features of the thermodynamic function at small baryon chemical potential are calculated through various representations using partition functions such as quark number susceptibility and Taylor's coefficients at around small chemical potentials in addition to other thermodynamic parameters [12].

So, in this paper, we calculate the thermodynamic properties of two-flavor magnetised PNJL model introducing thermal mass term in which a finite chemical potential is introduced due to the presence of finite chemical potential in the system. To fulfill our studies, we try to see the effects of relevant thermodynamic quantities like EOS using the chemical potential-dependent thermal quark mass and magnetised field introduced in the PNJL model. The proposal for the consideration of the magnetic field and chemical potential-dependent thermal mass in this calculation is due to the success of our earlier work on mPNJL model and probably QGP system is involved with large magnetic field as predicted by the experiments going on in RHIC and LHC [13]. However, the introduction of chemical potential is necessary as a large number of charged particles are present. So, these charged particles produce effective magnetic field and due to this, there is an obvious consideration of magnetic interaction in Lagrangian [14,15].

The paper is arranged as follows: In §2, Lagrangian density of the system including the chemical potential and electromagnetic field in the Lagrangian with the addition of PNJL model is explained thoroughly. In §3 all the thermodynamic properties to determine the EOS of QGP are described with their relations. In §4, we give our numerical solutions of all these parameters as the

results. At last, we give the conclusion with the detailed information about the formation of QGP under the influence of chemical potential-dependent thermal mass and magnetising potential model with PNJL potential.

2. Lagrangian density of the magnetised PNJL model with chemical potential

In this section, we describe the formalism of PNJL model with the incorporation of magnetic field and non-zero chemical potential in the Lagrangian density. There are many works on the formalism of PNJL model reporting about the interacting potential in the Lagrangian density [16]. One of these studies is Polyakov loop potential which is the upgradation of the NJL model. These studies had given the details about the characteristic features of QCD phase structure. The PNJL model attempts to describe the most significant phenomena of the QCD called deconfinement and chiral symmetry breaking. To enhance the characteristic features of the PNJL model, the magnetic field and finite chemical potential are included as the interacting potential in the Lagrangian and as the chemical potential is involved in the system, the mass of the quark is also affected by this chemical potential. So, we consider the effective quark mass as the chemical potential-dependent thermal quark mass. Yet the introduction of these two magnetic and finite chemical potentials will produce similar characteristic features of its QCD phase structure and in other way, it may produce the changes in the feature of characteristic properties. Now the Lagrangian density in the presence of magnetic field and non-zero chemical potential is defined as before [17]:

$$\begin{aligned} \mathcal{L} = & \bar{\psi} (i\gamma_\mu D^\mu - m \pm \mu\gamma^0)\psi \\ & + \frac{G}{2} [(\bar{\psi}\psi)^2 + (\bar{\psi}_1\gamma_5\tau\psi)^2] \\ & - U(\eta^*, \eta, T) - \frac{1}{4} F_{\mu\nu} F^{\mu\nu}, \end{aligned} \tag{1}$$

where

$$\begin{aligned} U(\eta^*, \eta, T) = & -\frac{1}{2} b_2(T) \eta^* \eta + b_4(T) \ln[1 - 6\eta^* \eta \\ & + 4(\eta^{*3} + \eta^3) - 3(\eta^* \eta)^2] \end{aligned} \tag{2}$$

in which

$$\begin{aligned} b_2(T) = & a_0 + a_1 \frac{T_0}{T} + a_2 \frac{T_0^2}{T^2}, \\ b_4(T) = & b_4 \frac{T_0^3}{T^3}, \end{aligned} \tag{3}$$

where the coefficients have the values $a_0 = 3.51$, $a_1 = -2.41$, $a_2 = 15.22$ and $b_4 = -1.75$ which are predicted

by lattice with the possible QCD features. $U(\eta, \eta^*, T)$ is the effective Polyakov loop interaction potential used in the Lagrangian density and the potential defines the dynamics of the field $\eta = Tr_c(L)/3$ and its conjugate $\eta^\dagger = Tr_c(L^\dagger)/3$ [18]. The potential $U(\eta, \eta^*, T)$ obeys the centre symmetry behaviour as in pure gauge QCD Lagrangian. However, it brings a similar solution in terms of the predicted result by the lattice for the entire behaviour of the Polyakov loop of the field η and the potential $U(\eta, \eta^*, T)$ has an absolute minimum at $\eta = 0$ with small temperature. However, the minimum value of $\eta = 0$ would be shifted to a finite value of η when the system has a temperature slightly higher than the critical temperature. Moreover, if temperature T tends to infinity, then the field η goes to unity. In such a situation, we choose the simplest possible effective potential, namely in the polynomial form of η and η^* [19]. So, the thermodynamical potential for the two-flavor quarks in the presence of chemical potential-dependent thermal quark mass and magnetic field is slightly modified with chemical potential and written as [20]

$$\begin{aligned} \Omega(\eta, \eta^*, m; T, \mu) = & U(\eta, \eta^*, T) \\ & + \frac{[m(T, \mu) - (m_0 \mp \mu)]^2}{4G} \\ & - 2N_f eBT \sum_{\nu=0}^{\infty} (2 - \delta_{0\nu}) \left[\int_0^\infty dp_z E_p \frac{2}{\pi^3} \right. \\ & - 2 \int_0^\infty dp_z \frac{p_z^2}{\pi^2} [Tr \ln(1 + Le^{(E_p - \mu)/T}) \\ & \left. + Tr \ln(1 + L^\dagger e^{-(E_p - \mu)/T})] \right] - \frac{3(qB)^2}{2\pi^2} \\ & \times \left[\zeta'(-1, x_f) - \frac{1}{2}(x_f^2) - x_f \ln(x_f) + \frac{x_f^2}{4} \right] \end{aligned} \tag{4}$$

in which

$$x_f = \frac{M_f^2}{2q_f B},$$

$$\zeta'(-1, x_f) = \left. \frac{d\zeta}{dz} \right|_{z=-1},$$

where $\zeta(z, x_f)$ is the Reimann–Hurwitz zeta function.

In the above formula

$$E_p = \sqrt{(p_z^2 + m^2(T, \mu) + 2enB) \pm \mu}$$

is the Hartree single quasiparticle energy. It is evaluated through the chemical potential-dependent thermal quark mass with n representing the number of Landau levels [21]. The chemical potential $\pm\mu$ represents the quark and antiquark. In the quasimodel technique, the mass of

the quark is considered as temperature-dependent. Here, we consider the effect of the chemical potential in the mass of the quark as the system of QGP is considered in the presence of a large number of charge particles. So, we cannot neglect the effect of chemical potential in the thermal quark mass. This kind of chemical potential dependency of the thermal mass is obtained elsewhere also [22]. Therefore, the mass is being taken as temperature- and chemical potential-dependent and it substitutes the role taken by the quark mass. However, it is a simple model calculation, only the consideration in the system is high temperature and imbalanced number of particles between the particles and antiparticles. Due to this imbalanced particles, chemical potential is created among the particles. Besides these information of charge particles, we found the study of QCD phase transition in which the properties of paramagnetic effect are taken care of. These properties are dependent on the temperature and chemical potential. Furthermore, increasing the magnetic field strength increases the magnitude of thermodynamic quantities. The magnetic effect also enhances the chiral symmetry breaking leading to increasing critical temperature for the chiral restoration phase. So, this simple model of chemical potential-dependent thermal quark mass tries to explain the same features of QCD structure as produced by other researchers. However, it looks at the improvement over other works. So it is defined as

$$m^2(T, \mu) = 16\pi\gamma_{qg}\alpha_s(E_p)\left(T^2 + \frac{\mu^2}{\pi^2}\right) \quad (5)$$

in which

$$\gamma_{qg} = \frac{\sqrt{2(\gamma_g^2 + \gamma_q^2)}}{\gamma_g\gamma_q}$$

with $\gamma_g = 6\gamma_q$ and $\gamma_q = \frac{1}{6}$.

Then the constant values used in the expression are the same as we used earlier in the study of QGP formation. In the QGP formation, these values give the most stable droplets. So we fixed it as the most suitable parameter for the present calculation.

$\alpha_s(E_p)$ is defined as the running coupling constant which is an indirect function of the magnetic field. The strength of this coupling also decreases with increase in magnetic field. It is defined in terms of the energy cut-off and QCD parameter Λ as

$$\alpha_s(E_p) = 4\pi/\left[(33 - 2n_f)\ln\left(1 + \frac{E_p^2}{\Lambda^2}\right)\right].$$

The energy cut-off is represented by E_p which is used to control the divergence of the system and QCD parameter Λ is 150 MeV. In general, the fields η and η^* are

different at non-zero quark chemical potential indicated by ref. [23]. It also explains primarily the consequence as quantum fluctuations of the fields around their mean field value. Considering the influence of the external magnetic field in the system, we look at the structure of QCD phase diagram evaluating all the thermodynamic properties of the system. The chemical potential introduced in thermal mass and the effect of the magnetic field increase the chiral condensate due to the widening of the gap between the Landau levels, increasing the low-energy contributions to the chiral condensate [24]. This chemical potential further forwards the process of suppression of the quark condensate due to the strong screening effect of the gluon interactions in the region of the low momenta relevant for the chiral symmetry breaking mechanism [25]. The suppression of quark condensate represents inverse magnetic catalysis (IMC), representing itself in the decreasing function and the opposite action of the pseudocritical chiral transition temperature in the Polyakov loop [26]. But, if we look at the case of the NJL model, the quarks interact through local current–current couplings, assuming that the gluonic degree of freedom can be frozen into point-like effective interactions between the quarks. So, some mechanisms to fulfill the structure of QCD phase diagram were worked out [27]. These mechanisms are used for introducing the initial temperature T_0 in the Polyakov loop potential [28,29]. Moreover, PNJL model couples with G_s connecting through the running coupling constants [30,31]. Due to this, it can decrease the effects of magnetic field allowing to contribute the effects of α_s .

3. Thermodynamic properties of the magnetised PNJL model with chemical potential

We briefly explain all the thermodynamic parameters of QCD, say pressure, energy density, entropy density, number density and susceptibility. These bulk thermodynamic parameters are obtained from the above definition of thermodynamic potential. The thermodynamic potential is incorporated by the chemical potential and magnetic field. The pressure in terms of standard thermodynamic relation is obtained as functions of temperature and chemical potential [32]:

$$P(T, \mu) = -\Omega(T, \mu). \quad (6)$$

Then we use the relation to calculate the energy density as

$$\epsilon(T, \mu) = -T^2 \frac{\partial \frac{\Omega(T, \mu)}{T}}{\partial T}. \quad (7)$$

From this formula, the energy density of the model in which the chemical potential is involved in the

Lagrangian density and the interacting potential incorporated with non-zero magnetic field is obtained. It means the properties of the PNJL model are evaluated with the chemical potential and non-zero magnetic field. Similarly, the entropy density of the system is also determined to investigate the equilibrium state and the disordered state of the system. However, the definition of entropy is defined on the basis of the first and second-order derivatives of the Gibbs potential function. Therefore, entropy density as a function of temperature and chemical potential is given by the relation

$$s(T, \mu) = -\frac{4}{3}T \frac{\partial \Omega}{\partial T}. \tag{8}$$

In a similar fashion we calculate the number density and it gives the information of the fluctuation of particle contribution. The fluctuations of particles are obtained only when the system has chemical non-equilibrium. In such situations, particle fluctuation arises due to the imbalance in the presence of particles and antiparticles in the system. So we can relate the number density through the thermodynamic potential with the change of chemical potential. So it is given as

$$\eta_q(T, \mu) = -\frac{\partial \Omega(T, \mu)}{\partial \mu}. \tag{9}$$

Now after finding the number density, it is understood that there is an imbalance of particles in the system. Due to this imbalance in particle contribution, there is no neutrality in charge contribution. So, charge contribution can account in determining magnetic susceptibility. The susceptibility measurement is now attributed by the movement of these particles inside the QGP system. Whether it is large or small is measured by calculation using the relation obtained through the Gibbs potential. So, the susceptibility is obtained as the second derivative of thermodynamic potential with respect to the chemical potential which is defined as the standard relation in many literatures.

$$\chi_\mu(T, \mu) = -\frac{\partial^2 \Omega(T, \mu)}{\partial \mu^2}. \tag{10}$$

Again, the Taylor coefficients C_2 and C_4 are determined to fulfill the complete QCD phase structure. These coefficients are used by Karsch *et al* and they used it by expanding around a small finite value. In these relations, they use the general technique of Taylor expansions from which C_2 and C_4 can be determined. So, we calculate these values to represent the pattern and behaviour of QCD structure.

$$C_n = \frac{1}{n!} \frac{\partial^n p(T, \mu)/T^4}{\partial (\mu/T)^n}. \tag{11}$$

From this relation, we obtain the relevant values of second- and fourth-order coefficients. These fitted values of the Taylor’s coefficients show the dependence of coefficients on the temperature. Therefore, a maximum term of the polynomial up to the fourth order of finite chemical potential is taken as the suitable choice in the numerical approximation. Then we consider these two coefficients in comparison to other authors works. In figures 6 and 7, these coefficients are demonstrated and represented in comparison with the zero chemical potential result as a function of temperature. So all the calculated thermodynamic properties with the inclusion of chemical potential and magnetised PNJL model in Lagrangian density give the entire information about the strongly interacting matter of QGP. The fourth-order calculation indicates in the approximation order of the coefficient with the consideration of their limitation in the numerical accuracy.

4. Results

This work is an extension of our earlier work on PNJL model by including the non-zero chemical potential and magnetic field in the Lagrangian density [33]. In the result, the QCD phase diagram is highlighted. In this phase diagram, the structure of the QCD is discussed by considering the chemical potential in thermal mass and non-zero magnetic field in Lagrangian density with the PNJL model. By using the thermodynamic relations, we study phenomenologically the bulk thermodynamic parameters by changing the temperature at different values of chemical potential for a particular value of magnetic field. The choice of a particular value of magnetic field is just to take care of the entire range of large magnetic field. So we did not choose the least and large value of magnetic field. Instead, we choose an approximate average value of the entire range of magnetic field.

First of all, we plot the QCD phase structure in figure 1. We plot this graph for three values of magnetic fields at the minimum, average and almost maximum average values. All other plots will lie in between these plots and the results can be summarised in such a way that they have a similar pattern with a slight change in the transition pattern. The structure is obtained at large values of chemical potential, say a range of $\mu = 200$ to 900 MeV. Large chemical potential produces large magnetic field and at larger values of magnetic field, the transition is faster and it is visible at larger temperature whereas at zero magnetic field and slightly lower value from the average magnetic field at 1.2 GeV^2 , it takes longer time and the temperature is lower than the transition temperature at maximum magnetic field. With the introduction of magnetic field, the transition temperature is found to

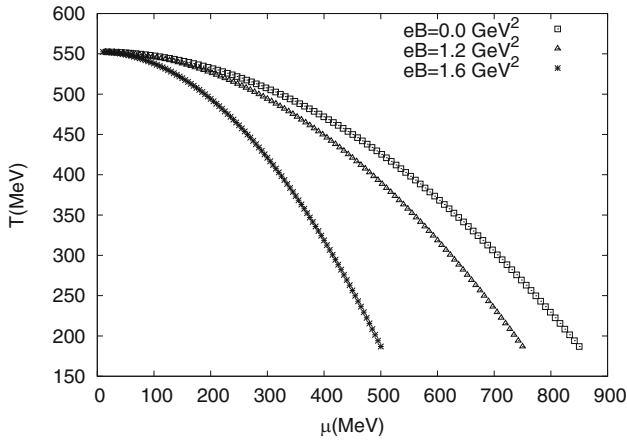


Figure 1. $T-\mu$ graph when $eB = 0, 1.2$ and 1.6 GeV^2 .

be higher. It is indicated by the phase transition shown in figure 1. So the structure can describe the features of QCD in nature.

In figure 2, we plot energy density as a function of temperature at finite different chemical potentials μ introduced in the thermal mass and non-zero magnetised PNJL model. The figure gives the energy density of different chemical potentials and zero chemical potential. If we look at the magnitude of energy density at a particular temperature, say T_c , the energy densities of the minimum and average zero chemical potentials are almost equal to the energy density of zero chemical potential up to the temperature $T = 1.6T_c$, whereas the value of the energy density for chemical potential $\mu = 300$ is much higher than the lower value of chemical potential. It means that the contributed particles are mainly from free coloured quarks–antiquarks and gluons. When the temperature is raised beyond such a point of the critical temperature, there is an abrupt change in the energy density at the range of lower temperature and then goes to the constancy in its value of energy density when the temperature is reached around $2.2T_c$. During this energy density expansion, the state of the matter is completely composed of colour unbound free quarks and gluon whereas when the critical temperature is below 170 MeV the state of such matter is contributed by colourless bound state of quarks. Again, we look at the changes of energy density at different chemical potentials at one particular magnetic field $eB = 1.2 \text{ GeV}^2$. With the increase of the chemical potential from $\mu = 0$ to finite value $\mu = 300 \text{ MeV}$, the energy density calculated with the model correspondingly increases from the initial temperature to a finite temperature $T = 2.2T_c$. The increment is faster for the temperature range of $T = 0-2.2T_c$. The constancy in the energy density is reached after $T = 2.2T_c$ for all values of μ .

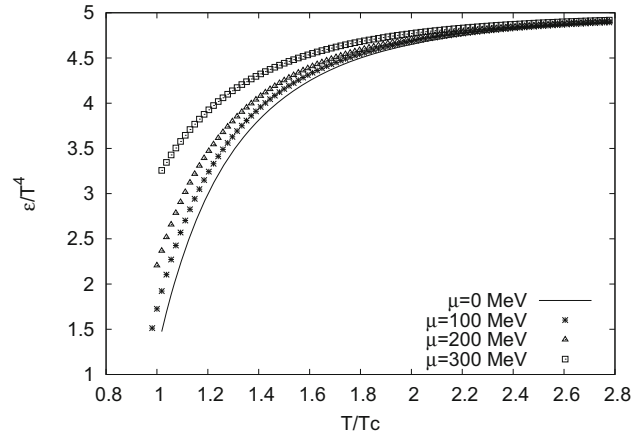


Figure 2. Energy density as a function of temperature when $\mu = (0, 100, 200, 300) \text{ MeV}$ at a fixed magnetic field value of $eB = 1.2 \text{ GeV}^2$. When $\mu = 0$, the result is from *Euro. J. Phys. C* **49**(1), 213 (2007).

In the same way, in figure 3 the pressure shows a similar behaviour with the energy density up to the temperature around $2.2T_c$ and this phenomenon is already known from the thermodynamic relation between pressure and energy density as given by $P = \epsilon/3$. The only difference of magnitude can be identified by one third of the energy density. It implies that it shows enhancement in the pressure up to the temperature $2.2T_c$ after incorporating non-zero magnetic field and finite chemical potential in the thermal mass introduced in the PNJL model. It then reaches a constancy of pressure and the same with the other results of earlier works when the temperature is raised beyond it.

Figure 4 shows the plot of the entropy density with the variation of temperature, for different values of chemical

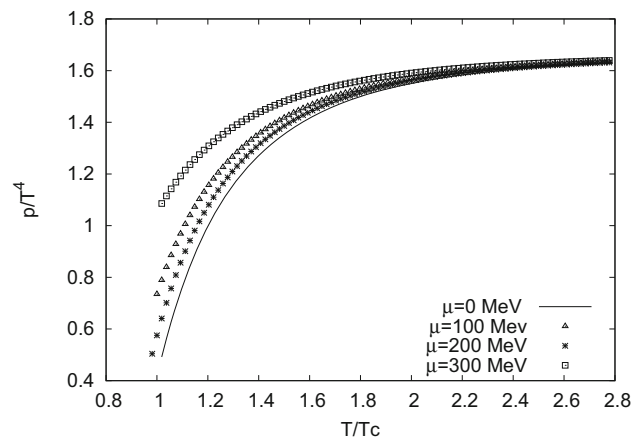


Figure 3. Pressure as a function of temperature when $\mu = (0, 100, 200, 300) \text{ MeV}$ at fixed magnetic field value of $eB = 1.2 \text{ GeV}^2$. At $\mu = 0$, the result is from *Eur. J. Phys. C* **49**(1), 213 (2007).

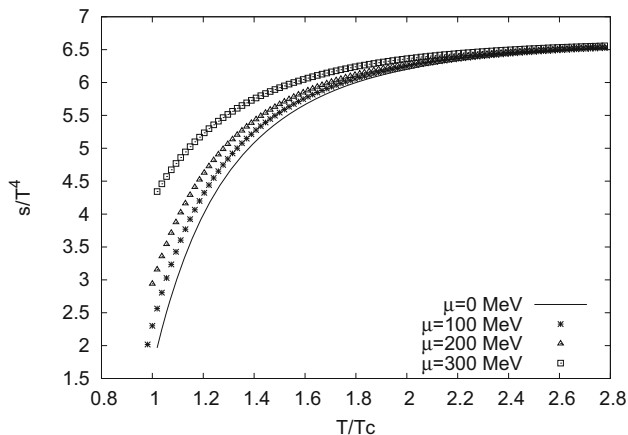


Figure 4. Entropy as a function of temperature when $\mu = (0, 100, 200, 300)$ MeV at a fixed magnetic field value of $eB = 1.2 \text{ GeV}^2$. When $\mu = 0$, the result is from *Euro. J. Phys. C* **49(1)**, 213 (2007).

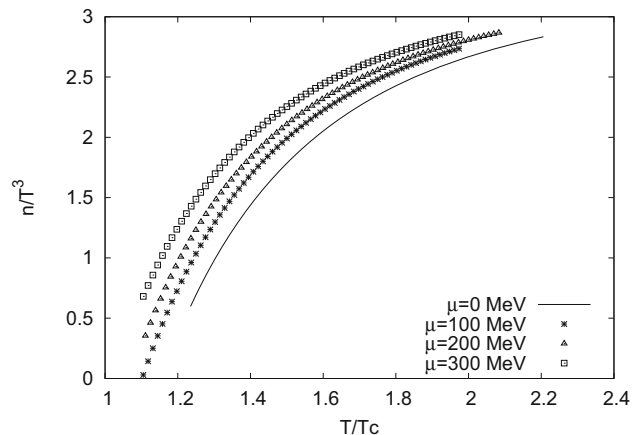


Figure 5. The number density as a function of temperature when $\mu = (0, 100, 200, 300)$ MeV at a fixed magnetic field value of $eB = 1.2 \text{ GeV}^2$. When $\mu = 0$, the result is from *Eur. J. Phys. C* **49(1)**, 213 (2007).

potential introduced in the thermal mass from $\mu = 0$ to 350 MeV and non-zero magnetic field at $eB = 1.2 \text{ GeV}^2$. We observed the enhancement in the value of entropy density with increasing chemical potential up to $\mu = 300 \text{ MeV}$. The increment in the value of entropy density is faster up to $T = 2.2T_c$, then it shows constancy in the behaviour of entropy density. We can say that the effect of non-zero magnetic field and chemical potential in thermal mass is effective up to $2.2T_c$ and disappear after this temperature. However, entropy density is the measurement of the phase transition of QGP as first- and second-order phases. This type of standard definition can be obtained by the first and second derivative of the Gibbs potential function.

In figure 5, we calculate the number density with temperature at non-zero magnetic field and chemical potential of the model. The result almost follows the pattern of the predicted lattice, indicating the enhancement in behaviour of the number density after the inclusion of non-zero chemical potential in the thermal mass and magnetic field in the PNJL model. It implies that the system has deconfinement of more free quarks and gluons with increasing temperature in comparison with low temperature where all the particles are confined in hadrons.

Then, we calculate the susceptibility for these incorporated non-zero magnetic field with chemical potential in the thermal mass of the PNJL model. The result of model calculation is demonstrated in figure 6. The figure follows increments following the similar pattern of lattice behaviour and the result shows much improvement over the earlier outputs [34]. The enhancement is found for the change of chemical potential μ , say from 0 to 300 MeV with the increase of temperature up to

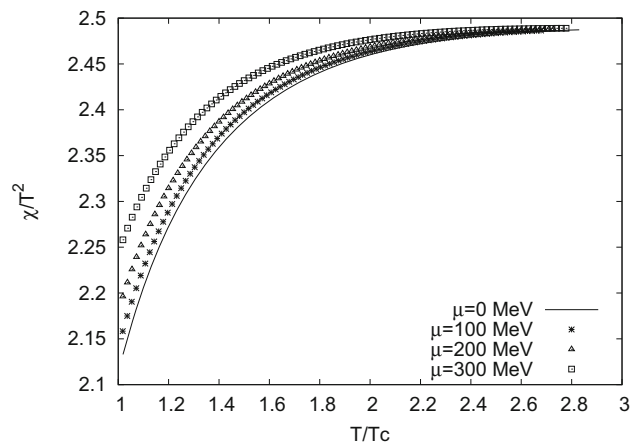


Figure 6. The susceptibility as a function of temperature when $\mu = (0, 100, 200, 300)$ MeV at a fixed magnetic field value $eB = 1.2 \text{ GeV}^2$. When $\mu = 0$, the result is from *Eur. J. Phys. C* **49(1)**, 213 (2007).

$T = 2.2T_c$. With the increase of μ beyond 300 MeV , the result is almost the same in the susceptibility calculation for the entire range of temperature. It means the effects of non-zero magnetic field and chemical potential in the thermal mass are saturated reaching the threshold value of $\mu = 300 \text{ MeV}$ and temperature around $T = 2.2T_c$. Obviously, the improvement is due to the effect of the chemical potential in thermal mass and non-zero magnetic field present in the PNJL model. It implies that such a simple model with a slight modification introducing the non-zero magnetic field in the PNJL model shows very much trivial and linear solution up to the temperature $T = 1.4T_c$ with the introduction of the non-zero magnetic field in the PNJL model. The improvement in the phase structure of number

density and susceptibility using non-zero magnetic field and chemical potential in thermal mass indeed shows the picturisation of good enhancement in comparison to the phase structure with only thermal mass and the magnetised PNJL model. However, the modification in Gibbs potential with the non-zero magnetic field and chemical potential in thermal mass with PNJL model may result in magnetic catalysis which is obtained due to the quark condensate enhancement and there may be the inverse magnetic catalysis which is due to the suppression of quark condensation in the system [35,36]. These processes are reversed to the NJL model where gluonic degree of freedom are frozen into point-like effective interaction among quarks only.

However, we added a new comparative graph in figure 7 in which we compare the data of Ratti, Abuki *et al* and our model [37]. In the other works, it is considered with zero quark mass whereas in our work we use the thermal and chemical potential-dependent quark mass. From the figure, it is observed that using thermal mass and non-zero chemical potential in the mass, enhance the output of susceptibility. It indicates that the model we used can explain the susceptibility with increased result.

In figures 8 and 9, the second- and fourth-order coefficients of Taylor expansion are shown [38]. The calculation of these coefficients enables one to control the continuum and infinite volume extrapolations through the coefficient basis. Moreover, these coefficients cannot be disturbed by thermodynamic polarity because the expectation value of the thermodynamic parameters are used most of the times.

So, the calculated results are the most expected and predicted one when we considered the PNJL model in calculating the QCD thermodynamics at different chemical potentials μ .

Figure 8 shows the second-order coefficient for various values of chemical potential in the thermal mass with the change of temperature. The coefficient increases with variation of temperature for lower values of chemical potential from $\mu = 0$ to 100 MeV. Then, on increasing the chemical potential, the coefficient starts increasing more at the beginning, say around $1.6T_c$ and after this temperature the coefficient increment is much narrower for the entire temperature range. It is due to the fact that the coefficient has lesser effect with large contribution from chemical potential and the coefficient becomes almost similar after reaching some threshold value of μ as 300 MeV. If we keep on increasing the chemical potential, the effects of non-zero magnetic field and chemical potential start disappearing. Moreover, in calculating the fourth-order coefficient, the Taylor coefficients are found to be varying and these characteristic features are also obtained in earlier calculations.

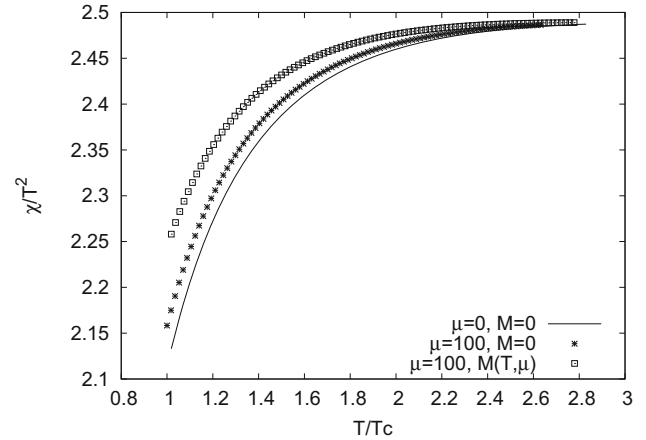


Figure 7. The susceptibility as a function of temperature when $\mu = (0, 100)$ MeV at a fixed magnetic field value $eB = 1.2 \text{ GeV}^2$. When $\mu = 0$, the result is from *Eur. J. Phys. C* **49**(1), 213 (2007). For $\mu = 100 \text{ MeV}$, $M = 0$, the result is from *Phys. Rev. D* **78**, 034034 (2008). For $\mu = 100 \text{ MeV}$, $M(T, \mu)$, the result is from our model.

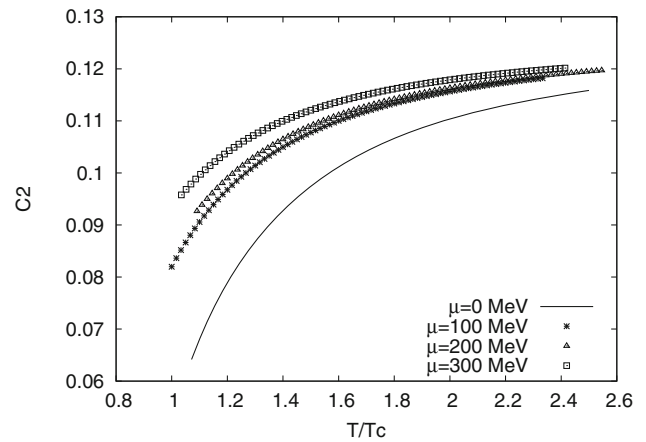


Figure 8. The Taylor coefficient of second-order function of temperature when $\mu = (0, 100, 200, 300)$ MeV at a fixed magnetic field value of $eB = 1.2 \text{ GeV}^2$. When $\mu = 0$, the result is from *Eur. J. Phys. C* **49**(1), 213 (2007).

In figure 9, the results are compared with the corresponding data produced by other models of zero magnetic field, which is considered without the effect of thermal mass and magnetised potential.

However, in figure 10 we show the comparative plots of pressure with temperature for three masses when $eB = 1.2 \text{ GeV}^2$. The plot for temperature- and chemical potential-dependent mass shows a uniformly a large increment in comparison to the thermal-dependent mass and quark mass. The subsequent increment in pressure is visible up to $T = 2.5T_c$ and the value of pressure is approximately the same beyond this temperature. The result shows that the model explains empirically in a

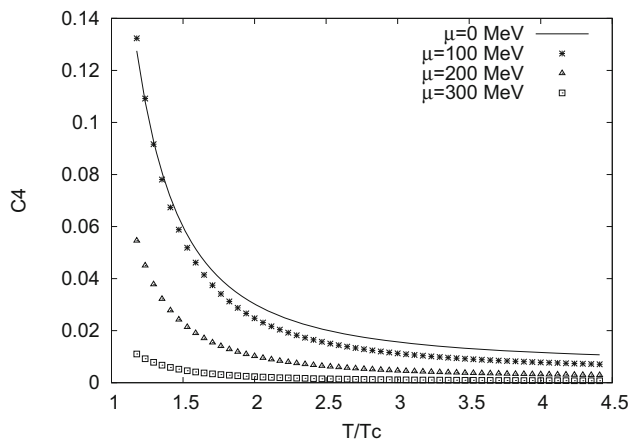


Figure 9. Fourth-order Taylor coefficient as a function of temperature when $\mu = (0, 100, 200, 300)$ MeV at a fixed magnetic field value of $eB = 1.2 \text{ GeV}^2$. When $\mu = 0$, the result is shown in *Eur. J. Phys. C* **49**(1), 213 (2007).

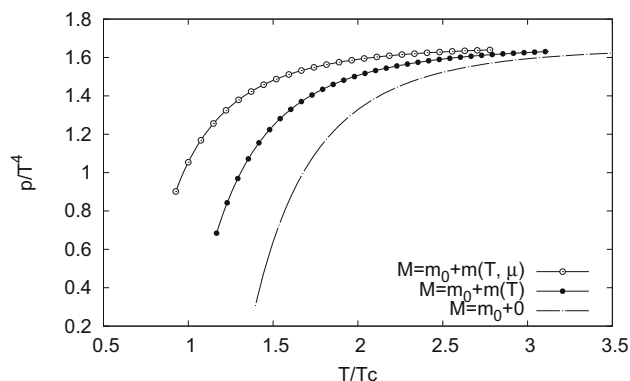


Figure 10. p/T^4 as a function of temperature for different masses when $eB = 1.2 \text{ GeV}^2$.

good pattern about the QCD phase structure by considering temperature- and chemical potential-dependent mass as a simple model. Therefore, it indicates that the present model of non-zero magnetic field and chemical potential introduced in thermal mass is quite capable of describing the QCD phase structure.

5. Conclusion

The NJL model has successfully explained the results of two-flavor QCD thermodynamic parameters. The result states the improvement with the results obtained from other calculations. Now Polyakov loop is an extended calculation of NJL model and the model can reproduce two-flavor thermodynamic properties. The coupling of quarks to the Polyakov loop produces a statistical suppression in thermodynamical properties of the one- and two-quark flavor model. We successfully implemented

the PNJL model with the inclusion of chemical potential in the thermal mass and it is considered in the presence of magnetic field B in the PNJL model [39]. The thermodynamic behaviour at zero and finite chemical potentials has been determined and analysed using Polyakov loop potential and different cross-over criteria are shown. More sophisticated fit functions seem to be necessary to reproduce the correct behaviour at finite chemical potential. Furthermore, in the two-flavor PNJL model, we analysed a speciality of QCD structure at finite chemical potential. The PNJL model predicts different critical temperature for the phase transition and their difference increases as the strength of the magnetic field increases. However, there is a prediction of PNJL model about the different critical temperatures and its increment of transition temperature with the increase of magnetic field [40,41]. The increase in transition temperature due to the presence of magnetic field is also obtained from the running coupling constant that the magnetic field is indirect function with it. The magnetic field factor involved in the energy of the system is given in the expression of running coupling constant. It is inversely proportional to the coupling constant, and so it has an impact on the transition temperature. So, the transition temperature increases slightly with the chemical potential and no evidence for a disentanglement of phase transition was found, at least for magnetic fields. To have the details about the magnetic effects, the model was initiated to modify the PNJL model separately in our first calculation without chemical potential. Then we again slightly changed the thermal mass making it temperature- and chemical potential-dependent. By changing this parameter, we look at the changes in the thermodynamic behaviour of QCD, earlier found by many researchers. We found the thermodynamic results of our model as enhanced from the results obtained by other researchers and it is closer to the results of Stefan–Boltzmann’s behaviour by introducing this model of chemical potential-dependent thermal mass and magnetic field. Moreover, this type of mechanism can also push up the transition to first order at low values of magnetic field. So, the effective model of QCD has accounted a lot in the features of both chiral symmetry breaking and de-confinement by using the effective potential obtained in pure gauge sector. The presence of chemical potential-dependent thermal mass and magnetic field can explain the formation of QGP and it can describe the structure of QCD in a meaningful way [42]. Therefore, it can be concluded that chemical potential with magnetised PNJL model can form QGP beyond the temperature, $T = 170 \text{ MeV}$. So phase transition can be obtained at temperature $T = 170\text{--}200 \text{ MeV}$ with the chemical potential and non-zero magnetic field. In the calculation, we also assumed and took the same value

of transition temperature used by Ratti so that the whole calculations are easier than the other models [43]. As the temperature is raised, the intensity will be increased from the predicted lattice data [44–47].

Acknowledgements

The authors thank the retired Prof. R Ramanathan for his untiring work in helping us for the manuscript's preparation and writings. His discussions help in fulfilling the manuscript preparation. The author, Anju thanks the University and CSIR, Delhi for providing financial supports in terms of Senior Research Fellowship (SRF) for this work.

References

- [1] Najmul Haque, *Proc. Indian Natl Sci. Acad.* **81**, 86 (2015)
- [2] P N Meisinger and M C Ogilvie, *Phys. Lett. B* **379**, 163 (1996)
- [3] C Ratti, M A Thaler and W Weise, *Phys. Rev. D* **73**, 014019 (2006)
- [4] H Hansen, W M Alberico, A Beraudo, A Molinari, M Nardi and C Ratti, *Phys. Rev. D* **75**, 065004 (2007)
- [5] K Fukushima, *Phys. Rev. D* **77**, 114028 (2008)
- [6] A N Tawfik and Niseem Magdy, *Phys. Rev. C* **90**, 015204 (2014)
- [7] A N Tawfik and Niseem Magdy, *Phys. Rev. C* **91**, 015206 (2015)
- [8] A N Tawfik and Abdel Magied Diab, *Eur. Phys. J. A* **57**, 200 (2021)
- [9] L Adamczyk *et al*, *Phys. Rev. Lett.* **114**, 252302 (2015)
- [10] S R Oner, C Ratti and W Weise, *Phys. Rev. D* **75**, 034007 (2007)
- [11] P Costa, C A de Sousa, M C Ruivo and Y L Kalinovsky, *Phys. Lett. B* **647**, 431 (2007)
- [12] J Moreira, B Hiller, A A Osipov and A H Blin, *Int. J. Mod. Phys. A* **27**, 1250060 (2012)
- [13] Evan Stewart and Kirill Tuchin, *Phys. Rev. C* **97**, 044906 (2018)
- [14] S Gupta, N Kartik and P Majumdar, *Phys. Rev. D* **90**, 034001 (2014)
- [15] Z F Cui, Y L Du and H S Zong, *Int. J. Mod. Phys: Conf. Ser.* **29**, 1460232 (2014)
- [16] K Fukushima and M Ruggier, *Phys. Rev. D* **81**, 114031 (2010)
- [17] A N Tawfik, A M Diab and M T Hussein, *J. Phys. G* **45**, 055008 (2018)
- [18] F Karsch, *AIP Conf. Proc.* **842**, 20 (2006)
- [19] S Lawley, W Bentz and A W Thomas, *J. Phys. G* **32**, 667 (2006)
- [20] K Fukushima, *Phys. Lett. B* **591**, 277 (2004)
- [21] S S Singh and Y Kumar, *Can. J. Phys.* **92**, 31 (2014)
- [22] V M Bannur, *Eur. Phys. J. C* **50**, 629 (2007)
- [23] Y Nambu and G J Lasinio, *Phys. Rev. B* **124**, 246 (1961)
- [24] S P Klevansky, *Rev. Mod. Phys.* **64**, 649 (1992)
- [25] P Wang, A W Thomas and A G Williams, *Phys. Rev. C* **75**, 045202 (2007)
- [26] A M Polyakov, *Phys. Lett. B* **72**, 477 (1978)
- [27] A Gocksch and M Ogilvie, *Phys. Rev. D* **31**, 877 (1985)
- [28] M Fukugita and A Ukawa, *Phys. Rev. Lett. B* **57**, 503 (1986)
- [29] S K Ghosh, T K Mukherjee, M G Mustafa and R Ray, *Phys. Rev. D* **73**, 114007 (2006)
- [30] K Kashiwa, H Kouno, M Matsuzaki and M Yahiro, *Phys. Lett. B* **662**, 26 (2008)
- [31] C Ratti, S Roessner and W Weise, *Phys. Lett. B* **649**, 57 (2007)
- [32] G S Bali, F Bruckmann, G Endro di, Z Fodor, S D Katz and A Schafer, *Phys. Rev. D* **86**, 071502 (2012)
- [33] A Dahiya and S S Singh, *Pramana – J. Phys.* **94**, 120 (2020)
- [34] Hong Mao, Jinshuang Jin and Mei Huang, *J. Phys. G* **37**, 035001 (2009)
- [35] P R Subramanian, H Stocker and W Greiner, *Phys. Lett. B* **173**, 468 (1986)
- [36] M G Alford, K Rajagopal and F Wilczek, *Nucl. Phys. B* **537**, 443 (1999)
- [37] H Abuki, R Anglani, R Gatto, G Nardulli and M Ruggieri, *Phys. Rev. D* **78**, 034034 (2008)
- [38] Y Hatta and T Ikeda, *Phys. Rev. D* **67**, 014028 (2003)
- [39] M Ferreira, P Costa, D P Menezes, C Providencia and N N Scoccola, *Phys. Rev. D* **89**, 016002 (2014)
- [40] D H Rischke, D T Son and M A Stephanov, *Phys. Rev. Lett. B* **87**, 062001 (2001)
- [41] D Blaschke, S Fredriksson, H Grigorian, A M Oztas and F Sandin, *Phys. Rev. D* **72**, 065020 (2005)
- [42] N D Ippolito, G Nardulli and M Ruggieri, *JHEP* **0704**, 036 (2007)
- [43] Y Aoki, Z Fodor, S D Katz and K K Szabo, *JHEP* **0601**, 089 (2006)
- [44] K Fukushima, *Phys. Rev. D* **69**, 097502 (2009)
- [45] P G Allen and N N Scoccola, *Phys. Rev. D* **88**, 094003 (2013)
- [46] P G Allen, V Pagura and N N Scoccola, *Phys. Rev. D* **91**, 114024 (2015)
- [47] C R Allton *et al*, *Phys. Rev. D* **71**, 054508 (2005)